

# Chapter 6

## Fractals

### Literature

- J. SCHMELZER, G. RÖPKE, and R. MAHNKE, *Aggregation Phenomena in Complex Systems: Principles and Applications*, J. Wiley (1999) + References.
- D. STAUFFER and AMONON AHARONY it Perkolationsstheorie, VCH (1995).
- M.F. BARNSLEY, R.L. DEVANEY, B.B. MANDELBROT, H.O. PEITGEN, D. SAUPE, and R.F. VOSS, *The Science of Fractal Images*, Springer (1988).
- H. GOULD and J. TOBOCHUK, *An Introduction to Computer Simulation Methods: Application to Physical Systems, Part II*, Addison Wesley (1988).

### 6.1 Introduction

Before the invention of computers fractals have come up twice as an important question. The first time was when British map makers discovered the problem with measuring the length of Britain's coast. On a zoomed out map, the coastline was measured to be about 5,000 something or other (in some odd units). But, anyway, by measuring the coast on more zoomed in maps, it got to be longer, like 8,000. And by looking at really detailed maps, the coastline was beyond twice the original. You see, the coastline of Britain that's on a map of the world doesn't have all the bays and harbors. A map of Britain has more of these, but not all the little coves and sounds.

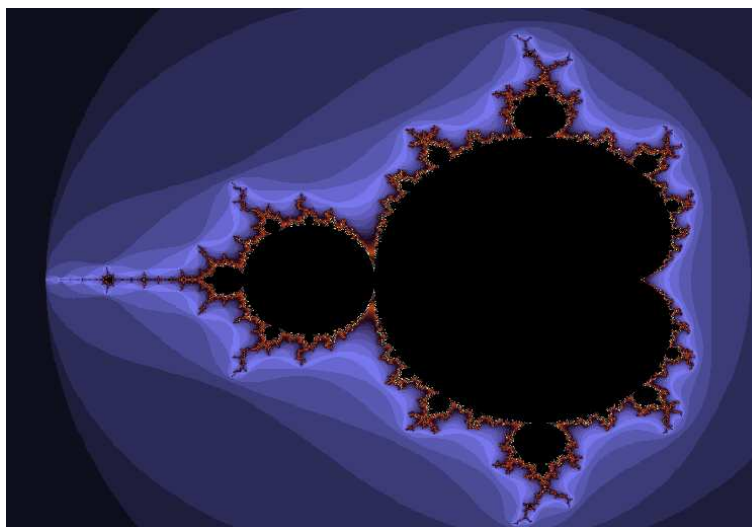


Figure 6.1: A typical MANDELNBROT fractal.

The closer they looked, the more detailed and longer the coastline got. (A finite area, aka Britain, being surrounded by an infinite line.)

The second instance of pre-computer fractals was noted by French mathematician G. JULIA. He wondered what a complex polynomial function would look like, such as the ones named after him, in the form of  $z^2 + c$ , where  $c$  is a complex constant. The idea behind the formula is that you take the  $x$  and  $y$  coordinates of a point and plug them into  $z$  in the form  $z = x + iy$ , square this number and then add  $c$ , a constant. Then plug the resulting pair of real and imaginary numbers back into  $z$ , run the equation again, and keep doing so until the result is greater than some number, the 'orbit'. The number of times you have to run the equations to get out of its 'orbit' can be assigned a color and then the pixel  $(x, y)$  gets turned into that color, unless those coordinates can't get out of their orbit, in which case they're made black.

Later, B. MANDELNBROT, an employee of IBM, thought about writing a program with a formula such as  $Z(n)^2 + c$  and then running it on IBM's many computers. They eventually got some pretty pictures. (See, for instance, Fig. 6.1.) He also coined the notion *fractal*.

The basic concept of fractals is that they contain a large degree of *self similarity*. This means that they usually contain little copies of themselves buried deep within the original and they also have infinite detail. Like the costal problem, the more you zoom in on a fractal, the more detail (coastline) you get.

A wide variety of natural objects does not have well-defined and simple geometric shapes. Examples can be found in plants, sea shells, polymers, thin films, colloids,<sup>1</sup> and aerosols. Often these structures have un-

---

<sup>1</sup>*Colloid*: a substance consisting of very tiny particles that are usually between 1 nanometer and 1000 nanometers in diameter and that are suspended in a continuous

usual, but pleasing shapes.

We will see that these unusual figures have non integer dimensions. Some geometric objects are exact fractals with the same dimension for all their points, while for other objects the dimension can be defined only locally or on the average. We will not study the theories that lead to fractal geometry, but we will rather look at how some simple models and rules produce fractal structures. To the extent that these models generate structures like those occurring in nature, it is reasonable to assume that the natural processes must be governed by similar rules. There are many physical systems exhibiting fractal structures, but the detailed study would go beyond the scope of the present lecture note.

Consider a common abstract "object" such as the charge density of an atom. There are an infinite number of ways to measure its "size", for example: each moment of the distribution provides a measure of the size, and there are infinite numbers of moments. Likewise, when we deal with complicated objects that have fractional dimensions, there are different definitions of dimension conceivable, and each may give a somewhat different answer. In addition, the fractal dimension is often defined by using a measuring box the size of which approaches zero. In realistic applications there is in general a smallest and a largest scale, respectively, which also hampers the precise determination of the fractional dimension.

Our first definition of a fractional dimension  $d_f$  (or HAUSDORF dimension  $d_H$ ) is based on our knowledge that a line is of dimension 1, a rectangle dimension 2, and a cube dimension 3. Let's assume we have a mathematical formula, that yields results in agreement with our experience for regular objects. It seems perfectly legitimate, then, to apply this formula to fractal objects, resulting in non-integer values for  $d_f$ . For simplicity, let us consider objects that have the same length  $L$  on each side, as do equilateral triangles and squares. We postulate that the dimension of an object is determined by the dependence of its mass upon its length.

$$M(L) = AL^{d_f}. \quad (6.1)$$

Here  $A$  is a constant and the power  $d_f$  is the fractal dimension. As you may verify, this rule works with the regular figures of our experience, so it must make some sense. Yet we will see that when we apply it to some unusual objects, this rule produces fractional values for  $d_f$ .

Fractals have technological applications. Antennas have always been a tricky subject. The usual long, thin wires aren't the best way. Antenna arrays, another approach, consist of thousands of small antennas which are either placed randomly or regularly spaced. Fractals provide the perfect mix between randomness and order, and with fewer components. Parts of fractals have the disorder, while the fractal as a whole provides the order. Fractal antennas can now be found in many mobile phones and they are

---

medium, such as a liquid, a solid, or a gaseous substance.

approximately 25% more effective than traditional antenna designs. They are also cheaper and can operate multiple bands because for an antenna to work equally well at all frequencies it must be symmetrical around a point and must be self-similar, both of which fractals can provide.

## 6.2 The SIERPINSKI Gasket

We generate our first fractal, shown in Fig. 6.2, by placing dots on a plane according to the following rules

1. Draw an equilateral triangle with vertices  $P_1, P_2,$  and  $P_3$ .
2. Place a dot at an arbitrary point  $P = (x_0, y_0)$  within the triangle.
3. Choose an integer  $i \in \{1, 2, 3\}$  at random and place a dot halfway between  $P$  and vertex  $P_i$ .
4. Keep repeating step 3 upon using the last dot as the new  $P$ .

---

### Algorithm 13 MATLAB Code: SIERPINSKI Gasket

---

```
function X = sierp_fct(P,N_pts)
rx = rand(1,1)*.5;
ry = rand(1,1);
if (ry > 2*rx)
    rx = rx + .5; ry = 1-ry;
end
X = zeros(N_pts,2);
X(1,:) = [rx ry];
n = unidrnd(3,[N_pts,1]);
    % integer random number from {1,2,3}
for i = 2: N_pts
    X(i,:) = (X(i-1,:) + P(n(i),:))/2;
end
return

%-----

N_pts = 50000;
P = [0 0; 1 0; .5 1; 0 0];
X = sierp_fct(P,N_pts);
plot(P(:,1),P(:,2),'-k');
hold on
plot(X(2:end,1),X(2:end,2),'.k','markersize',1);
drawnow;
```

---

After 50000 points, one obtains a collection of dots like in Fig. 6.2.

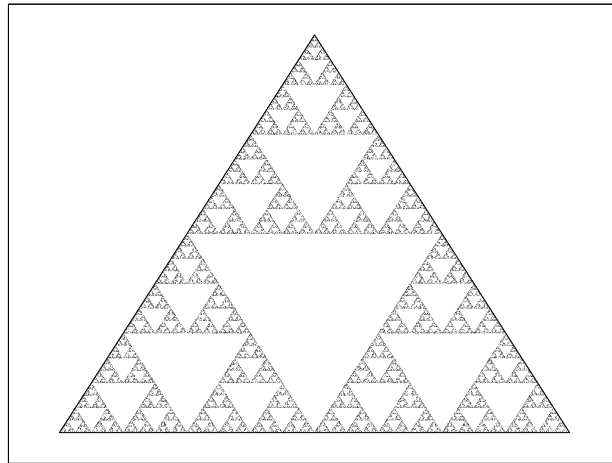


Figure 6.2: A SIERPINSKI gasket containing 50000 points. This pattern has been found in the tile work of medieval monasteries and on the shells of sea animals. Each filled part of this figure is self-similar.

---

**Algorithm 14** MATLAB Code: Fractal Dimensions

---

```

N_pts = 15000;
N_rep = 100;
L = 10; N = 2^L;
alpha = zeros(N_rep,1);
for ir = 1: N_rep
    X = sierp_fct(P,N_pts);
    X = ceil(X*N); % map onto grid
    A = zeros(N,N);
    A(sub2ind([N,N],X(:,1),X(:,2))) = 1;
    for i = 1: L
        LL(i) = 2^i;
        m(i) = sum(sum(A(1:LL(i),1:LL(i))));
    end
    ind = find(m > 0);
    ln_LL = log(LL(ind));
    ln_m = log(m(ind));
    [p,S] = polyfit(ln_LL,ln_m,1);
    alpha(ir) = p(1);
end
fprintf('alpha = %10.3f +/- %10.3f\n',...
        mean(alpha),std(alpha)/sqrt(N_rep));

```

---

The numerical result for the fractal dimension for a sample of size  $N_{\text{rep}} = 100$  reads

$$\alpha = 1.59 \pm 0.01.$$

## 6.3 Analytic Determination of the Fractal Dimension

The topology of Fig. 6.2 was first analyzed by the Polish mathematician SIERPINSKI. Observe that there is the the same structure in a small region as there is in the entire figure. In other words, if the figure were infinitely dense, any point of the figure could be scaled up in size and will be similar to the whole. This property is called **self-similarity**.

Another construction of the SIERPINSKI gasket is suggested by Fig. 6.2. Fill the original triangle with black color. Remove an inverted equilateral triangle of size  $L/3$ . The resulting figure consists of three black equilateral triangles. Keep on removing inverted triangles from the center of the filled triangles. At each iteration the figure contains filled triangles, all of the same size. Finally, we scale the figure up so that each filled triangle has the original size.

Next, we analyze how the density  $\rho = \frac{\text{mass}}{\text{area}}$  depends on size. Assume that each triangle has size  $r$  and mass  $m$ . The density of the single triangle reads:

$$\rho(L = r) = \frac{M = m}{r^2} \stackrel{\text{def}}{=} \rho_0.$$

Next, for the triangle with side  $L = 2r$  the density is:

$$\rho(L = 2r) = \frac{M = 3m}{(2r)^2} = \frac{3m}{4r^2} = \frac{3}{4} \rho_0.$$

We see that the extra white space leads to a density that is  $3/4$  the density of the previous stage. In the next step we obtain

$$\rho(L = 4r) = \frac{M = 9m}{(4r)^2} = \left(\frac{3}{4}\right)^2 \frac{m}{r^2} = \left(\frac{3}{4}\right)^2 \rho_0.$$

We see that as we continue the construction process, the density of each new structure is  $3/4$  the density of the previous one. This is unusual. For ordinary objects the density is an insensitive quantity, independent of the size of the object. For this strange object, there is a power-law dependence of the density on the size of the object

$$\rho = CL^\alpha,$$

where  $C$  is some constant. The power  $\alpha$  is determined via:

$$\alpha = \frac{\Delta \log \rho(L)}{\Delta \log(L)} = \frac{\log(1) - \log(3/4)}{\log(1) - \log(2)} = \frac{\log(3)}{\log(2)} - 2 \simeq -0.41504.$$

This means that, as the gasket gets larger and larger, it contains more and more open space. So even though its mass approaches infinity, its density approaches zero! And since a two-dimensional figure like a solid triangle has a constant density as its length increases, a 2D figure would have  $\alpha = 0$ . Since the SIERPINSKI gasket has a nonzero  $\alpha$  value, it is not a 2D object! The fractional dimension  $d_f$  is defined by

$$M(L) = \rho(L) * L^2 = CL^{\alpha+2} = CL^{d_f}.$$

Hence

$$d_f = \alpha + 2 \simeq 1.58496,$$

which is in perfect agreement with the numerical result. We see that the SIERPINSKI gasket has a dimension between that of a 1D line and a 2D triangle; that is, it has a fractional dimension.

## 6.4 Length of a Coastline

MANDELBROT asked the classic question "What is the length of the coastline of Britain?". MANDELBROT's answer introduces another definition to our study of fractals, namely using box counting to determine fractal dimension.

As illustrated in Fig. 6.3, the plane is divided into squares of size  $s$  and we count the number of cells  $N$  which are crossed by the object under consideration. Then the scale  $s$  is changed and the box counting is repeated leading to the dependence of the number of crossed cells  $N(s)$  on the scale  $s$ . For 1D objects, we have

$$N(s) \propto s^{-1},$$

and for 2D objects the relation is:

$$N(s) \propto s^{-2}.$$

The dimension  $d$  enters into the power law as

$$N(s) \propto s^{-d},$$

and we extend this formula to fractal objects.

The fractal dimension is then determined from a straight line fit to the  $N(s)$  data on a log-log scale. Points close to the scales  $s = 1$  and  $s = L$  have to be omitted, as the self-similarity breaks down at these points because the surface is constructed with a finite resolution  $s = 1$  and has finite size  $s = L$ .

Fig. 6.4 contains the fractal dimension  $d_f$  for different surfaces during the growth process. Due to the finite range of the surface, the fractal dimension is a random variable and varies during the growth process. The average fractal dimension is  $d_f = 1.22$ .

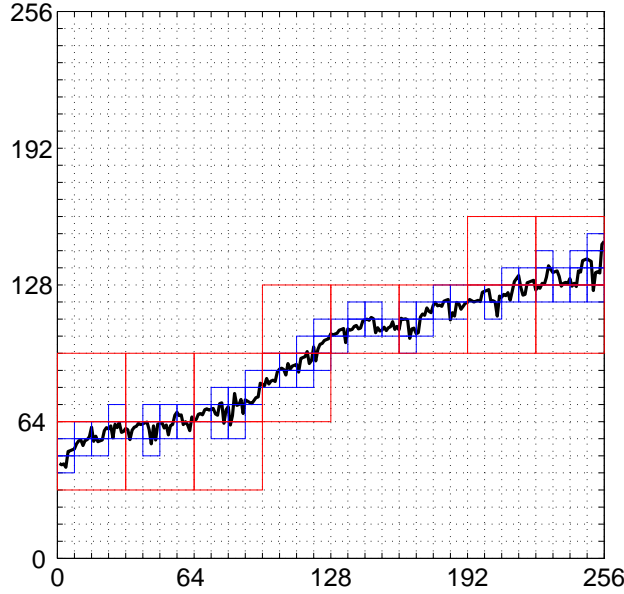


Figure 6.3: Illustration of the box counting method. The surface has been tilted to make the counting procedure more obvious. On scale  $s = 8$  the curve passes through  $N_8 = 70$  (blue) boxes, while  $N_{32} = 14$  (red) boxes are crossed on the scale  $s = 32$ .

## 6.5 Ballistic deposition

There is a number of physical processes in which particles are deposited on a surface to form a film. Here we consider particles that are evaporated thermally from a hot filament. The emission, the propagation to the surface and the diffusion on the surface are random processes. Nonetheless, the films produced by deposition turn out to have well-defined structures. We will simulate this growth process on the computer by simplified rules.

### Simulation

Consider particles falling onto and sticking to a horizontal line of length  $L$ . The emission and propagation process to the final destination on the surface is mimicked by the following rules.

1. Start with a flat substrate and zero film thickness  $h_i = 0; \forall i$ .
2. Determine at random the site  $i$  at which the particle(s) will stick eventually.
3. Decide how many particles shall be added to this place.

$$h_i = \begin{cases} h_i + 1, & \text{if } h_i \geq h_{i-1} \text{ and } h_i \geq h_{i+1}; \\ \max(h_{i-1}, h_{i+1}), & \text{otherwise} \end{cases}$$



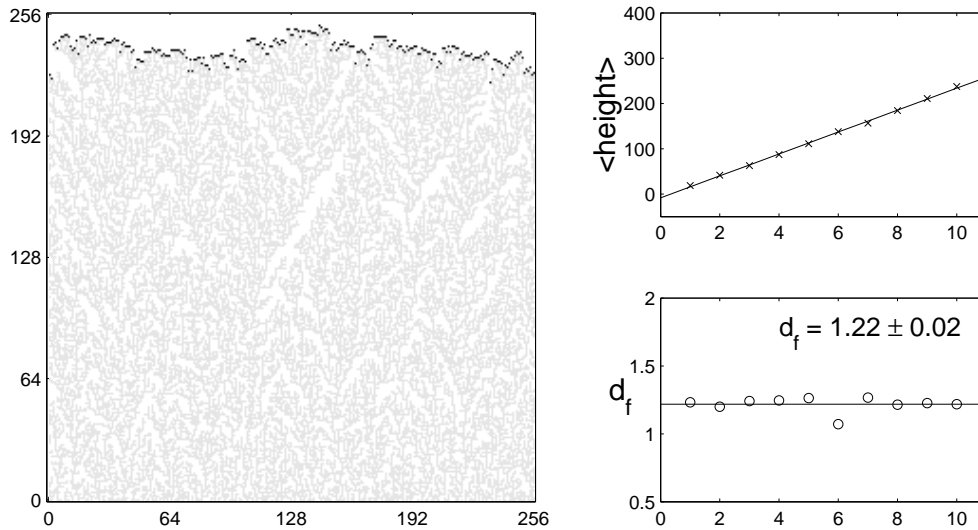


Figure 6.4: Simulation of the ballistic deposition on a 1D substrate (left panel). The top (black curve) represents the final surface. The other marks indicate heights, taken on during the growth process. The right panel shows the fractal dimensions of the surface during the growth process.

The reason for the last step is the acceleration of the time consuming diffusion process on the surface. The sticking probability is higher at edges than on plane surfaces patches. To model this effect, the height is increased by one if the particle lands on a flat surface patch, otherwise the height at site  $i$  is set to the maximum height of its neighbors.

A representative result of a simulation is shown in Fig. 6.4. We observe several randomly distributed empty regions in the figure on the left panel. They are a consequence of the plotting algorithm and have no physical meaning for the final film. Below the surface, which is indicated by black dots, all columns are completely filled. The fractal internal structure is a remnant of the growth process. Grey dots indicate surfaces of previous iterations. The empty parts of the columns occur when particles hit an edge, which is subsequently filled in one time step according to deposition rule (3). The average height increases linearly with time (see right panel of Fig. 6.4) and the surface has a fractal structure.

## 6.6 Diffusion-limited Aggregation

Diffusion-limited aggregation (DLA) takes place in non-living (mineral deposition, lightning paths) or living (corals) nature and results in objects with unusual geometry. We will first discuss the meaning of the terms in the notion 'DLA'.

Diffusion is a random motion of particles as has already been discussed in Sec. 1.4.2. Individual particles move typically far away from their original position. The distance, measured by the square-root of the variance, grows as:

$$d = \sqrt{\text{var}(\mathbf{x})} \propto \sqrt{t}.$$

In contrast to a normal flow, where all particles under consideration move more or less into the same direction, the average distance  $\langle \mathbf{x} \rangle$  covered by the particles within a random walk (Brownian motion) is zero. In diffusion there might be a net transport of material, when the starting density is not uniform. If you pour a drop of ink into a glass of water the ink spreads. But diffusion is not only a phenomenon in fluids, it can also occur in solids. It just takes much more time in the latter case.

The driving force for diffusion is the entropy. The energy of a state where all ink molecules are piled up in one corner could be the same as the energy for a state in which the ink is spread homogeneously. Consequently, each 'microstate' has the same statistical (BOLTZMANN-) weight. However, there are overwhelmingly more states supporting a homogeneous density than there are states yielding a significant inhomogeneity and the latter has vanishing odds to be observed.

Aggregations are formed, when particles attract each other and stick together. Depending on the strength of the forces the resulting aggregates differ. Strong forces lead to compact and well ordered crystalline structures. When the forces are weaker it may happen that particles stick together for a while and then travel around again. The resulting aggregates have no distinct shape. Each aggregate is unique. Fluffy, not compact, maybe tree like clusters emerge.

DLA-clusters are aggregates, where the shape of the cluster is controlled by the possibility of particles to reach the cluster. DLA-clusters are ideal objects for computer simulations. One approach is to simulate the random walk of the particles and their aggregation. Typically one uses a lattice, puts an initial seed particle at some origin and another particle somewhere on the lattice. Then the second particle moves around in random motion, step by step from lattice site to lattice site. Finally it will meet the first particle. Then another particle is thrown onto the lattice, it walks around and after a while meets the first two. This is continued for as many particles as one likes, one after the other.

There are many variations of the DLA model with more realistic properties depending upon the application of interest.

## Applications

DLA structures occur in the following applications:

- Exploitation of oil resources embedded in sand by means of water pressed into the sand. So water-oil-surface may or may not exhibit

shapes which resemble those of DLA.

- Catalyst forming. These materials of great value in chemical engineering may also show strongly branched surfaces with many holes and channels. The very large surface area is often relevant for the catalytic process.
- When metals like copper or gold are separated electrolytically out of a solution, shapes like DLA-cluster form under certain conditions.
- When metals are deposited onto surfaces from the gaseous phase to get very thin films a DLA-growth is observed.
- Deposition of carbon on the walls of a Diesel engine exhibit DLA structures.
- Generation of polymers out of solutions may follow a DLA-mechanism.

### Simulation

Here we study the most simple DLA simulation on a 2D lattice:

1. Define a simple square lattice of vacant grid points.
2. The linear size  $L$  of the lattice should be 'sufficiently large' in order to avoid boundary effects.
3. Place a seed particle (first element of the cluster) at the center of the lattice.
4. Draw a circle  $C_1$  that only just fits into the square and map it onto the grid points.
5. The points in and on  $C_1$  defines the area  $A_1$ .
6. Add a particle at random on  $C_1$ .
7. The particle performs a random walk with equal probability in the four nearest neighbor directions.
8. The random walk stops if
  - (a) the particle escapes from  $A_1$ .
  - (b) the particle touches the aggregate.  
Add the particle to the aggregate.
9. If the aggregate has not yet the desired size go to 6.

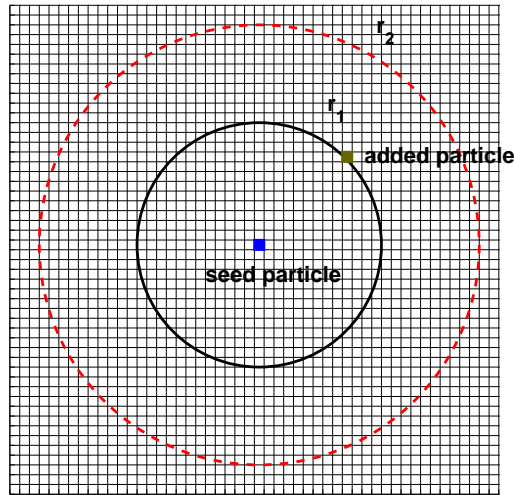


Figure 6.5: Setup of the DLA simulation.

In this form the algorithm is highly inefficient as it takes a long time until the particle eventually touches the aggregate. Since we are not interested in the dynamics itself but rather in the form of the aggregate, the simulation can be accelerated considerably due to the following reasoning. Consider a circle of radius  $r_1$  centered around the seed particle that is only slightly bigger than the aggregate at a given point in time. The situation is depicted in Fig. 6.5.

In order to reach the aggregate the random walk particle has to cross the circle. Due to symmetry, all points on the circle are crossed with equal probability. Hence, the particle can be added straight away somewhere on the circle with equal probability. This circle plays the role of circle  $C_1$  defined above. However, now we cannot stop the random walk if a particle leaves  $A_1$ . This would imply a bias since the escape probability is smaller on parts of the circle which are close to the aggregate than at parts which are far away. Therefore, we introduce an outer circle  $C_2$  of radius  $r_2 > r_1$  which defines the escape radius. If a particle crosses  $C_2$  it is lost and a new particle is added on  $C_1$ . Figure 6.6 shows a typical result of a DLA simulation .

The fractal dimension is determined analogously to the definition (6.1) via the mass  $M(s)$  or rather the density  $\rho(s)$ . Here it is sensible to consider the mass contained in concentric circles  $C(s)$  of radius  $s$  around the seed particle. The mass  $M(s)$  is defined as the number of aggregate cells inside the circle of radius  $s$ . The corresponding volume  $V(s)$  is the total number of cells within  $C(s)$ . The density reads  $\rho(s) = M(s)/V(s)$ . The fractal dimension is given by the power law dependence

$$M(s) \propto s^{d_f}.$$

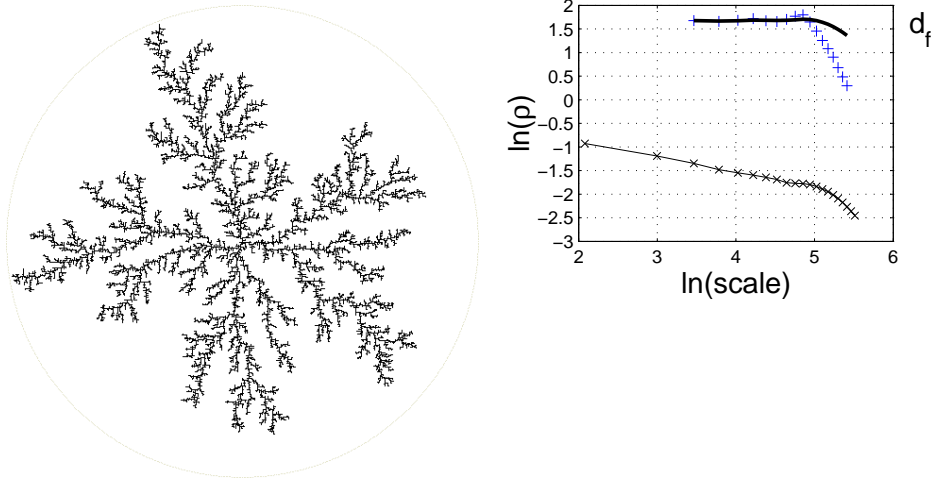


Figure 6.6: The left panel shows an aggregate with  $N = 16700$  particles on a grid of linear size  $L = 3000$  constructed with  $r_2/r_1 = 6$ . The right panel exhibits the density  $\rho$  as functions of scale  $s$  (lower curve) along with the local fractal dimension determined from the slope of 5 neighboring points and the cumulative average of the later.

In Fig. 6.6 we observe that the fractal dimension of the bulk of the graph is  $d_f \simeq 1.7$  while it decreases towards zero at the outer fringes. It is reasonable that the dimension decreases once the outer fringes of the aggregate are reached. A fractal dimension  $d_f = 0$  means that the mass is constant beyond a certain radius.

## 6.7 Percolation

### 6.7.1 Introduction

A representative question is as follows: Assume we have some porous material and we pour some liquid on top. Will the liquid be able to make its way from hole to hole and reach the bottom? We model this physical question mathematically as a three dimensional network of  $N^3$  points (or vertices). The connections (or edges) between each two neighbors may be open with probability  $p$  or closed with probability  $1 - p$ . What is the probability that an open path (open cluster) exists from top to bottom? (A *cluster* is a number of connected edges.) Mostly we are interested in the behavior for large  $N$ . As is quite typical, it is actually easier to examine an infinite network than just large ones. In this case the corresponding question is: Does there exist an infinite open cluster? Here we may use KOLMOGOROV's Zero-One Law (see Appendix C) to see that for any given  $p$  the probability that an infinite cluster exists is either zero or one. Thus,

there must be a *critical probability*  $p_c$  below which the probability for the existence of an open cluster is always zero and above which this probability is always equal to one.

Sometimes it is easier to open and close vertices rather than edges. This is called *site percolation* while the model described above is called *bond percolation*.

From all this we deduct that percolation is the simplest model for random media. One typical application is the simulation of the formation of gypsum. As percolation clusters can also be grown from one single seed, percolation gives rise to models for the spreading of epidemics.

### 6.7.2 The Model

We will argue the case on the basis of a site percolation model. For this purpose we investigate an alloy which consists of two components, atoms A and B. The concentration of A-atoms is described by  $p$  and both components are randomly distributed. Atom A carries a spin and there exists a short range magnetic interaction between next nearest neighbor A-atoms. B-atoms do not carry a spin. The alloy can only develop magnetic properties if an infinite net of connected A-atoms exists. Thus, we can assume that there exists a *critical concentration*  $p_c$  at which the alloy starts to develop magnetic properties and we observe a phase transition from non-magnetic to magnetic behavior.

Phase transitions can only be observed in infinite systems. In contrast, the computer only allows to study finite systems. But even for finite systems one will be able to observe a signature of the phase transition in the vicinity of  $p_c$ .

At small concentrations we expect to see only a number of small clusters of A-atoms in the sea of B-atoms and there will be no magnetic ordering. With increasing concentration  $p$  the average size of the clusters will increase until, at the critical value  $p_c$ , one cluster will spread across the whole sample. This is the *percolation cluster* or *infinite cluster*.  $p_c$  is the critical concentration or *percolation level*. For infinite sample size  $p_c$  is a well defined property and for a quadratic two-dimensional lattice with four nearest neighbors  $p_c = 0.59275 \pm 0.00003$  as was proved numerically. In a finite size system there will only be a certain probability - dependent on  $p$  - that an infinite cluster can exist.

There are many interesting properties besides the plain value of  $p_c$ . For instance, how does  $p_c$  depend on lattice symmetry or the percolation model? How does the average size of finite clusters change when  $p$  approaches  $p_c$  from below? How does the density of the infinite cluster increase for  $p > p_c$ ? Can one gain information on the distribution of the cluster size throughout the sample? What is the structure of the infinite cluster at  $p_c$ ?

Let us try to establish (without proof) a few concepts. We define, first of all, the average size  $R(s)$  of a cluster which consists of  $s$  elements using

$$R^2(s) = \frac{1}{s(s-1)} \sum_{i \neq j} (\mathbf{r}_i - \mathbf{r}_j)^2, \quad i, j = 1, \dots, s. \quad (6.2)$$

Here,  $i$  and  $j$  are indices which are used to identify the elements of the cluster and  $\mathbf{r}_i$  is the lattice position of element  $i$ . Thus, the average size  $\xi$  of a finite cluster is defined by

$$\xi = \sqrt{\langle R^2(s) \rangle_{s < \infty}}, \quad (6.3)$$

with  $\langle \dots \rangle_{s < \infty}$  the mean value over all finite clusters in the system.  $\xi$  diverges at  $p_c$  and close to  $p_c$  we have

$$\xi \sim |p - p_c|^{-\nu}. \quad (6.4)$$

This holds for all percolation models and  $\nu$  is an *universal critical exponent*. Universal means that  $\nu$  depends only on dimension, for instance in 2D one gets  $\nu = 3/4$  and for 3D a  $\nu \simeq 0.88$  is reported.

We introduce, furthermore, the probability  $P(p)$  that some arbitrary A-atom belongs to the infinite cluster. Obviously  $P(p) = 0$  for  $p < p_c$  because no infinite cluster exists. Thus,  $P(p)$  grows from  $P(p_c) = 0$  to  $P(1) = 1$ , and, again, close to  $p_c$

$$P(p) \sim (p - p_c)^\beta, \quad p \gtrsim p_c. \quad (6.5)$$

Here,  $\beta$  is another universal critical exponent; for 2D one gets  $\beta = 5/36 \simeq 0.14$ . Thus  $P(p)$  increases very rapidly.

The density  $p_c P(p_c)$  of the infinite cluster at  $p_c$  is, obviously, zero according to the above definition of  $P(p)$ . Nevertheless, the infinite cluster exists and it has a very interesting structure: it is a *fractal*. Thus, we introduce another item,  $M(L)$ .  $L$  is the linear dimension of a square clipping of the lattice and  $M(L)$  is the number of elements of the infinite cluster inside this square clipping. As the infinite cluster is a fractal at  $p_c$  we have

$$\langle M(L) \rangle \propto L^D, \quad p = p_c, \quad (6.6)$$

with  $\langle \dots \rangle$  the mean value over various clippings and  $D$  the fractal dimension. For 2D one gets  $D = 91/48 \simeq 1.89$  and  $D$  is an universal exponent.

There are many other properties of the system which develop exponential behavior close to the critical concentration. They are described by other universal critical exponents. Nevertheless, these singularities are not independent of each other as the theory of phase transitions based on renormalization group theory proves. They depend on each other via *scaling laws*.



We emphasized already that the critical exponents are defined only for infinite systems. On the other hand, the computer can handle only finite systems. There is no phase transition in such systems, no sharply defined critical concentration, and there are no divergencies. Is it possible to conclude from the properties of finite systems to the properties of the infinite system? The answer to this question is given by *finite scaling*.

Let  $M(p, L)$  be the average number of elements in a cluster which traverses a quadrat of linear dimension  $L$ . (This is the finite size equivalent of the infinite cluster.) For each value of  $L$  one can calculate  $M(p, L)$  as a function of  $p$  which results in a congruence of curves. Scaling theory of critical phenomena tells us that such a congruence of curves is close to the critical point described by one universal function  $f$  after appropriate scaling. The scale for  $M(p, L)$  and  $L$  can either be given in powers of  $p - p_c$  or using Eq. (6.4), in terms of  $\xi$ . Thus, we describe  $L$  in units of  $\xi$  and  $M(p, L)$  in units of  $\xi^x$ :

$$M(p, L) \sim \xi^x f\left(\frac{L}{\xi}\right). \quad (6.7)$$

Initially,  $f(L/\xi)$  is an unknown function and  $x$  is yet another critical exponent. We use  $L = k\xi$ , with  $k$  a constant, and get from Eq. (6.6)  $x = D$ . Thus, we measure  $L$  in units of  $\xi$  and  $M(p, L)$  in units of  $\xi^D$ . Consequently,

$$M(p, L) \sim \xi^D f(k), \quad (6.8)$$

or

$$\begin{aligned} \frac{M(p, L)}{L^d} &\sim \frac{\xi^D}{L^d} f(k) \\ &\sim \frac{\xi^D}{k^d \xi^d} f(k) \\ &\sim \xi^{D-d} f(k), \end{aligned} \quad (6.9)$$

with  $d$  the dimension of the system. Thus,  $L^d$  is the number of lattice points and  $M(p, L)/L^d$  is the probability for a lattice point to belong to the cluster under investigation. For large  $L$  we get:

$$\frac{M(p, L)}{L^d} \simeq pP(p) \sim (p - p_c)^\beta. \quad (6.10)$$

Using Eqs. (6.4) and (6.9) we, finally, arrive at

$$\begin{aligned} \frac{M(p, L)}{L^d} &\sim \xi^{D-d} f(k) \sim pP(p) \\ (p - p_c)^{\nu(D-d)} &\sim (p - p_c)^\beta, \end{aligned}$$

or

$$\beta = (d - D)\nu. \quad (6.11)$$



As a result, the three exponents  $D$ ,  $\beta$ , and  $\nu$  are linked by a scaling law.

This scaling law also helps in finding information on the dependence of the ‘singularities’ on the lattice size  $L$ . We use Eqs. (6.4) and (6.7) and get

$$\begin{aligned} M(p, L) \xi^{-D} &\sim f\left(\frac{L}{\xi}\right) \\ M(p, L) |p - p_c|^{D\nu} &\sim \tilde{f}[(p - p_c)L^{1/\nu}]. \end{aligned} \quad (6.12)$$

Thus, the concentration  $p$  and the system size  $L$  are linked close to the critical point ( $p = p_c$ ,  $L = \infty$ ).

In a first step we can determine the fractal dimension  $D$ . It has already been defined in Eq. (6.6). For  $L \ll \xi$  the finite system looks like the infinite system (self similarity of fractals) and we find using Eq. (6.6)  $M(p, L) \sim L^D$ . This enables us to calculate from the increase of the number of elements inside the infinite cluster,  $M(p_c, L)$ , with lattice size  $L$  numerically the fractal dimension  $D$ .

In order to determine  $p_c$  we develop another scaling law. Let  $\pi(p, L)$  be the probability for an infinite cluster to exist within a sample of size  $L$ . Thus,

$$\pi(p, \infty) = \begin{cases} 0 & p \leq p_c, \\ 1 & p > p_c, \end{cases}$$

in the infinite system. In finite systems this step function will become smoothed out. For  $L = \infty$  and  $p > p_c$   $\pi(p, \infty)$  is constant and the scale exponent has the value zero. Thus, we write in analogy to Eq. (6.12)

$$\pi(p, L) = g[(p - p_c)L^{1/\nu}], \quad (6.13)$$

with  $g(x)$  a still unknown function. Nevertheless, if we occupy the lattice sites with probability  $p$  and increase  $p$  the clusters will grow in size. At some level  $p_c(L)$  we will find an infinite cluster.

The probability to find  $p_c(L)$  within an interval  $[p, p + dp]$  is determined by the derivative  $(d\pi/dp)dp$  at  $p_c(L)$ . Obviously,  $d\pi/dp$  develops a maximum which diverges for  $L \rightarrow \infty$  and  $p_c(L) \rightarrow p_c(\infty)$ , the critical concentration of the infinite system. Because of statistical fluctuations, the maximum of  $d\pi/dp$  is rather hard to determine and it is advisable to calculate the mean value

$$\langle p_c(L) \rangle = \int dp p \frac{d\pi}{dp} \quad (6.14)$$

and the variance,  $\text{var}(p_c(L))$ . Eq. (6.13) results in the scaling law

$$\langle p_c(L) \rangle = \int dp p L^{1/\nu} g'[(p - p_c)L^{1/\nu}].$$

Using  $z = (p - p_c)L^{1/\nu}$  and  $\int dp (d\pi/dp) = \pi(1, L) - \pi(0, L) = 1$  (because for  $p = 1$  an infinite cluster exists independently of  $L$ ) we arrive at

$$\langle p_c(L) \rangle - p_c \sim L^{-1/\nu}. \quad (6.15)$$

---

**Algorithm 15** MATLAB Code: Simple Percolation

---

```
p = 0.5; % choose probability for A-atoms
L = 100; % choose lattice size
lat = zeros(L,L); % fill lattice with B-atoms
for i = 1:L
    for j = 1:L
        if rand(1) < p
            lat(i,j) = 1; % make A-atom
        end;
    end;
end;
end
```

---

If we now calculate  $p_c(L)$  for many simulations of a system of length  $L$  and if we repeat this for many other (big) values of  $L$  it will be possible to fit the mean value  $\langle p_c(L) \rangle$  to Eq. (6.15) which will result in values for  $p_c$  and  $\nu$ . Thus, the critical concentration  $p_c$  and the two exponents  $D$  and  $\nu$  have been determined using systems of finite size. Furthermore, applying the same algorithm to calculate  $\langle p_c(L)^2 \rangle$  will finally give for the variance:

$$\begin{aligned} \text{var}(p_c(L)) &= \langle p_c(L)^2 \rangle - \langle p_c(L) \rangle^2 \\ &= \langle [p_c(L) - p_c]^2 \rangle - \langle p_c(L) - p_c \rangle^2 \\ &\sim L^{-1/\nu}. \end{aligned} \tag{6.16}$$

Thus, the standard deviation of  $p_c(L)$  can be used to determine directly the critical component  $\nu$ .

### 6.7.3 The Algorithm

A simple algorithm is presented as Algorithm 15. It creates a random pattern of zeros (representing B-atoms) and ones (representing A-atoms) on a square lattice of linear dimension  $L$  for a given concentration  $p$  of A-atoms. We see that it is rather easy to generate the percolation pattern. The problem we are now confronted with is that we have to extract the desired information by ‘asking’ the appropriate questions.

First of all one needs an algorithm to identify clusters of connected lattice points. One possibility is to give cluster numbers to all occupied lattice sites with the provision that each lattice site which is not connected to a lattice site we have visited before receives a new cluster number. This method allows to visit each lattice site only once with the disadvantage that parts of the same cluster may be identified by different cluster numbers. At the end of the identifying algorithm these conflicts are resolved using book-keeping methods. A typical result is presented in Fig. 6.7 for a  $20 \times 20$  lattice and  $p = 0.5$ .

Finally, Fig. 6.8 demonstrates that the procedure discussed in the previous section which allows to derive the critical concentration  $p_c$  of the

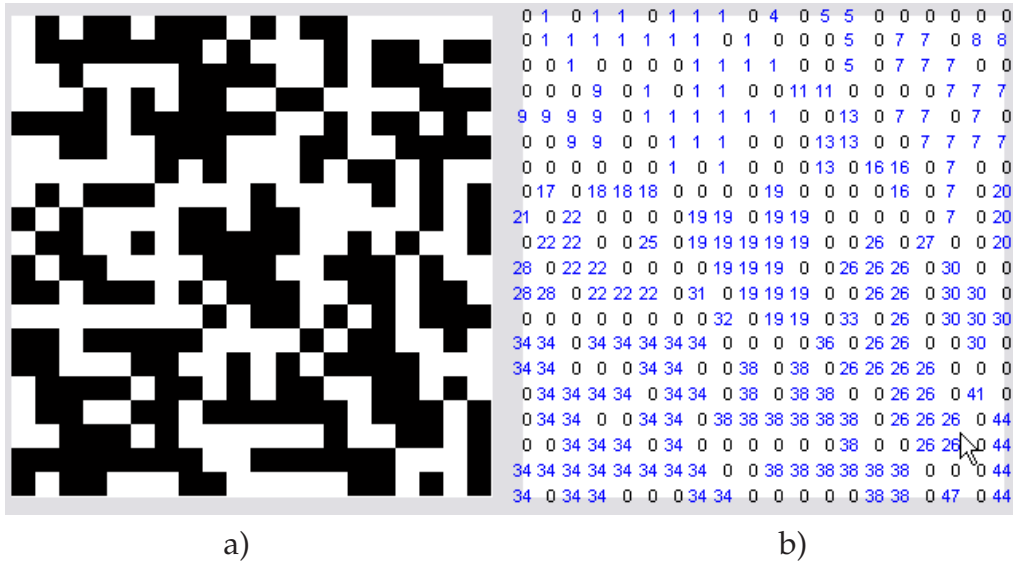


Figure 6.7: Frame a): A result of Algorithm 15 for  $p = 0.5$  on a square lattice with  $L = 20$ . Frame b): Lattice sites occupied by A-atoms identified by cluster numbers.

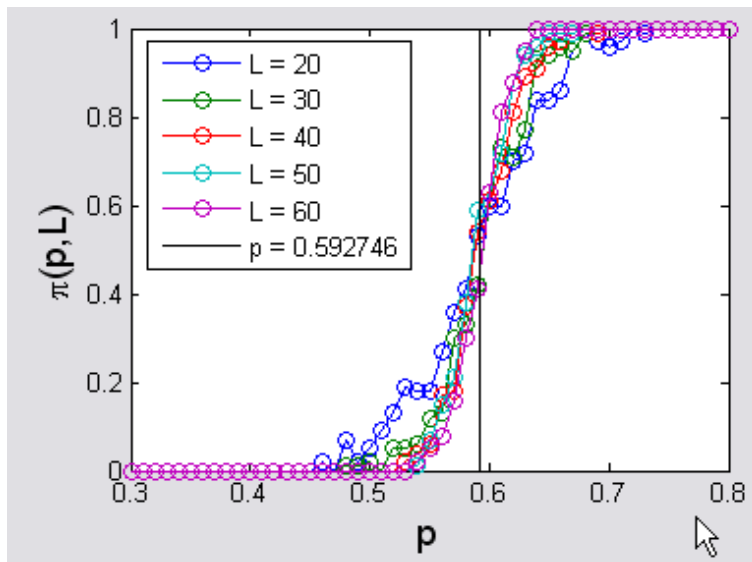


Figure 6.8:  $\pi(p, L)$  for a quadratic two-dimensional lattice. The black solid curve shows the critical behavior of the infinite sample. This graphs demonstrates the applicability of the procedure described above which allows to determine  $p_c$  from finite size samples only.

infinite system from finite size results only does indeed work. The figure shows the probability  $\pi(p, L)$  for an infinite cluster to exist within a sample of size  $L$ . The region in which  $d\pi/dp$  displays a maximum agrees well with the critical value  $p_c = 0.592746$  of the infinite system. We also see that the slope  $d\pi/dp$  close to  $p_c$  gets steeper with increasing lattice size  $L$ . The curves have been generated using 100 simulations per occupation probability  $p$ . All curves cross within a rather narrow region around  $\pi(p = 0.592746, L) = 0.5$ .